

Cite this: *J. Mater. Chem. B*, 2023, 11, 55Received 1st November 2022,
Accepted 5th December 2022

DOI: 10.1039/d2tb02386e

rsc.li/materials-b

Assembly of chemically modified protein nanocages into 3D materials for the adsorption of uremic toxins†

Hendrik Böhler,^a Setareh Orth-Alampour,^b Constance Baaten,^{bc} Maria Riedner,^d Joachim Jankowski^b and Tobias Beck^{ib*ae}

Hemodialysis fails to remove protein-bound uremic toxins that are attributed with high cardiovascular risk. Application of adsorption materials is a viable strategy, but suitable biocompatible adsorbents are still not available. Here, we demonstrate that adsorbents based on the bottom-up assembly of the intrinsically biocompatible protein cage ferritin are applicable for toxin adsorption. Due to the size-exclusion effect of its pores, only small molecules such as uremic toxins can enter the protein cage. Protein redesign techniques that target selectively the inner surface were used to introduce anchor sites for chemical modification. Porous crystalline adsorbents were fabricated by bottom-up assembly of the protein cage. Linkage of up to 96 phenylic or aliphatic molecules per container was verified by ESI-MS. Materials based on unmodified ferritin cages can already adsorb the uremic toxins. The adsorption capacity could be increased by about 50% through functionalization with hydrophobic molecules reaching $458 \mu\text{g g}^{-1}$ for indoxyl sulfate. The biohybrid materials show no contamination with endotoxins and do not activate blood platelets. These findings demonstrate the great potential of protein-based adsorbents for the clearance of uremic toxins: modifications enhance toxin adsorption without diminishing the biocompatibility of the final protein-based material.

About 50% of all fatalities in dialysis patients with end-stage CKD can be attributed to cardiovascular events linked to

impaired kidney function.¹ In recent years, many risk factors promoting cardiovascular diseases have been linked to protein-bound uremic toxins (PBUT).^{2,3} In clinical trials, it was shown that the PBUT *p*-cresyl sulfate (pCS) is associated with increased risk for cardiovascular and all-cause mortality in CKD patients.^{4–6} Additionally, pCS and other PBUTs such as indoxyl sulfate (IS) can induce kidney and renal fibrosis,^{3,7} inhibit endothelial proliferation,⁸ induce oxidative stress,⁹ and vascular calcification.^{6,10} Due to their hydrophobic character, a high fraction of the PBUTs is bound to plasma proteins, for example serum albumin, preventing an efficient diffusion through the pores of the dialysis membranes.^{11,12} Therefore, even with prolonged and more frequent sessions, common membrane-based dialysis techniques fail to sufficiently clear PBUTs from the blood.¹³ Several techniques for improving hemodialysis are under investigation, including the use of binding competitors,¹⁴ oral adsorbents,¹⁵ or synbiotika.¹⁶ A promising alternative method is the application of extracorporeal adsorbents.¹⁷ For easy and cost-effective broad-scale application, the adsorbent needs to possess a high bio- and hemocompatibility, allowing full-blood contact and simple integration in existing dialysis treatments.¹⁸ Some adsorption materials have been investigated for their ability of binding PBUTs such as zeolites,^{19,20} carbon-based materials,²¹ or zirconium-based metal-organic frameworks (MOF).²² However, only a few studies address the challenges in bio- and hemocompatibility during the application of these materials. Even if they do, the focus is on increasing the biocompatibility of conventional adsorption materials as recently demonstrated for activated charcoal.^{18,23} Instead of improving the biocompatibility of conventional adsorbents, starting with intrinsically biocompatible materials and increasing their binding affinity towards PBUTs is a promising alternative strategy. Here we report an unprecedented approach for the fabrication of a heterogeneous adsorbent for PBUTs. It is based on a bottom-up assembly strategy of protein cages with high intrinsic biocompatibility. We aim on answering two main questions.

^a Universität Hamburg, Department of Chemistry, Institute of Physical Chemistry, Grindelallee 117, Hamburg 20146, Germany. E-mail: tobias.beck@chemie.uni-hamburg.de

^b Universitätsklinikum Aachen, Institute for Molecular Cardiovascular Research IMCAR, Pauwelsstraße, 30, Aachen 52074, Germany

^c Maastricht University, Department of Biochemistry, Cardiovascular Research Institute Maastricht, Maastricht 6229 ER, The Netherlands

^d Universität Hamburg, Technology Platform Mass Spectrometry, Mittelweg 177, Hamburg 20148, Germany

^e The Hamburg Centre of Ultrafast Imaging, Hamburg, Germany

† Electronic supplementary information (ESI) available. See DOI: <https://doi.org/10.1039/d2tb02386e>



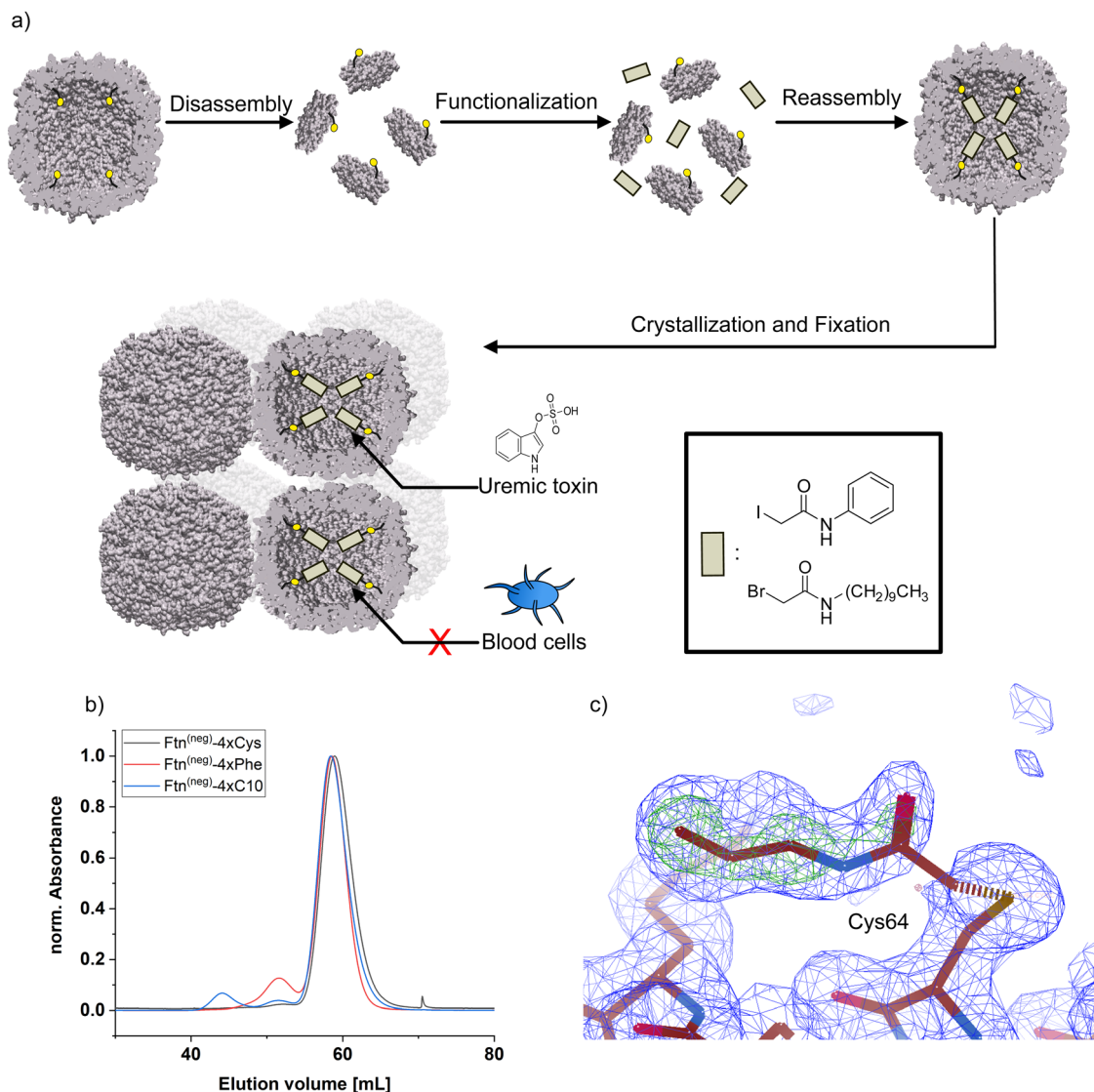


Fig. 1 (a) Schematic overview of the strategy for protein functionalization. Protein cage is disassembled into subunits and incubated with respective ligand. After reassembly, cages self-assemble into 3D-material and are chemical fixed. (b) Results from size-exclusion chromatography of ferritin before and after functionalization. (c) Electron density ($2F_{\text{O}}-F_{\text{C}}$ omit map, blue) and difference electron density ($F_{\text{O}}-F_{\text{C}}$, green) map for a functionalized cysteine residue with the (truncated) aliphatic molecule. $2F_{\text{O}}-F_{\text{C}}$ map (blue): 1 rmsd, $F_{\text{O}}-F_{\text{C}}$ (green): 5 rmsd. Maps were calculated without ligand atoms.

for the assembly of the protein cages to macroscopic materials are summarized in the next section.

By self-assembly of the protein cages, a well-defined crystalline material can be created with uniformly distributed solvent channels. We envisioned that this material structure ensures high purity of the material, comparability of different modified derivatives and accessibility of the cavities inside the material. Assembly into a macroscopic material with the protein cage as a building block is achieved by a batch crystallization technique. The general procedure is schematically shown in Fig. 2. The protein solution is cautiously mixed under constant shaking while adding the precipitant solution. After approximately 24 h, first crystals can be observed as shown in the left panel in Fig. 2. The size of the crystals can be tuned by altering protein and precipitant concentration (Fig. S11, ESI[†]). The protein

forms a cubic lattice in the space group $P23$ and possesses uniformly distributed solvent channels with a diameter of around 3 nm at its narrowest part (Fig. S12, ESI[†]).²⁹ To increase the stability, the crystals were fixated with a cross-linking agent. First experiments were conducted with glutaraldehyde. However, during stability tests in a 60 mg mL⁻¹ BSA solution, chosen to simulate the high protein content of the blood, the crystals dissolve (Fig. S13, ESI[†]). After an additional cross-linking step, the crystals tolerate the condition but the respective adsorption capacity is greatly diminished, which is probably due to the formation of oligomeric glutaraldehyde blocking the pores. Therefore, we chose a sulfo-SMCC cross-linker, which is unable to undergo reactions with itself (Fig. 2), allowing stable fixation by maintaining adsorption capacity. The sulfo-SMCC linker bears a maleimide group and an



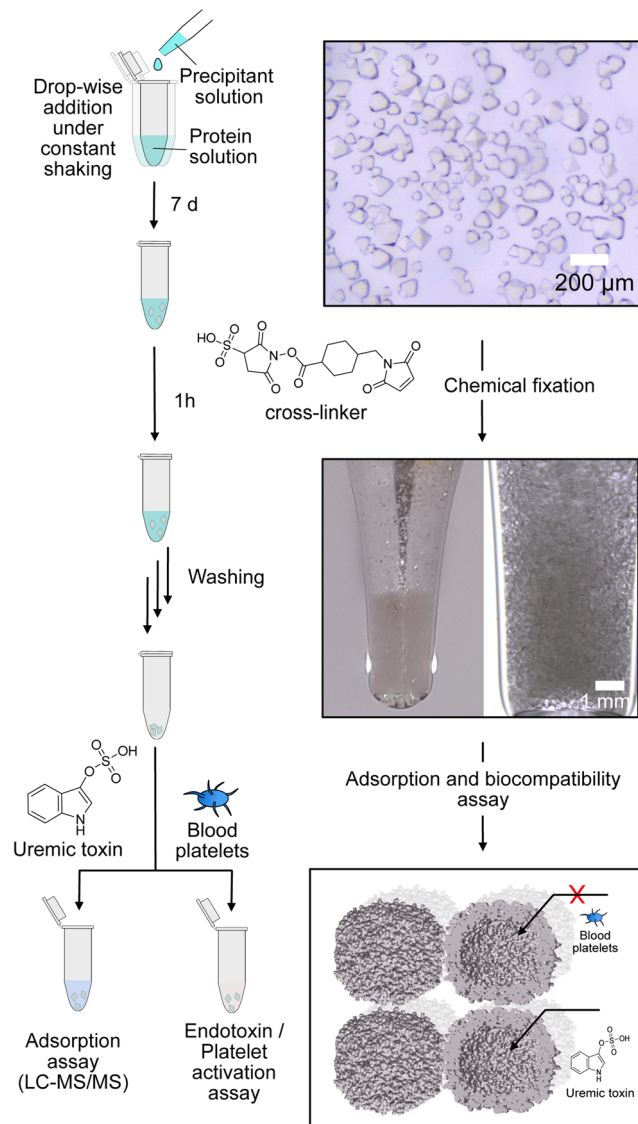


Fig. 2 Schematic overview of batch crystallization technique for fabrication of protein-based adsorption materials, images of the material before and after fixation and schematic depiction of the size-exclusion effect for excluding blood platelets from the inner cavity.

activated ester group. At the pH value of the mother liquor of pH 8.5, both groups can undergo reactions with the primary amine group of the amino acid lysine. The resulting crosslinks between different protein cages stabilize the crystal and increase its tolerance against aqueous solutions with high concentrations of BSA. Macroscopic crystalline materials from the functionalized variants could be fabricated under the same conditions, indicating that the functionalization did not influence the outer surface.

Subsequently, PBUT adsorption assays with the unfunctionalized protein-based material and the material functionalized with aliphatic or phenylic molecules were carried out. To this end, the respective sample was incubated in solutions of three different uremic toxins indoxyl sulfate (IS), *p*-cresyl sulfate (pCS), and phenylacetic acid (PheAc). Here, toxin

concentrations expected in an end-stage CKD patient were used.^{10,32,33} After incubation for 3 h, the PBUT concentration in the supernatant and respective control samples were determined by HPLC-MS/MS techniques. Finally, the protein-based material is vacuum-dried and weighed to determine the mass. The adsorption capacity, which is the ratio of the adsorbed mass of PBUT to the total mass of the material, is calculated and shown in Fig. 3.

Crystals of the unfunctionalized protein Ftn^(neg) adsorb all three tested toxins as seen in Fig. 3a–c with a capacity of 283 and 247 $\mu\text{g g}^{-1}$ for IS and pCS, respectively, and 2710 $\mu\text{g g}^{-1}$ for PheAc. The reason for the much higher capacity of the PheAc adsorption is most likely the 10-fold higher concentration of the PBUT in the assay (see above). For IS and pCS, functionalization with phenylic molecules (Phe) leads to an increase in adsorption capacity to 458 and 372 $\mu\text{g g}^{-1}$, respectively. However, based on statistical tests (see Fig. 3 and caption), only the capacity improvement for Ftn^(neg)-Phe with IS is significant. For functionalization with the aliphatic molecules (C10), the improvement of adsorption capacity is rather small (Fig. 3a and b). For the toxin PheAc, no significant enhancement of the adsorption could be observed after the incorporation of the hydrophobic molecules (Fig. 3c). The capacities of the protein-based adsorbent are in a similar regime but smaller than the values of other published materials, for example the P87 zeolites with capacities of up to 1000 $\mu\text{g mL}^{-1}$ ³⁴ or carbon-based adsorbents with capacities of up to 3200 $\mu\text{g mL}^{-1}$ ³⁵ with respect to IS. To the best of our knowledge, the adsorbent with the highest capacity published so far is a zirconium-based MOF with a capacity of up to 156 mg g^{-1} .²² However, efforts to install their biocompatibility need to be taken, which can further affect the adsorption capacity. On the other hand, our protein-based material approaches the problem from the other side: it has intrinsic biocompatibility, but its adsorption capacity can be further improved. Regarding this, capacities in the range of several hundred $\mu\text{g mL}^{-1}$ are a promising starting point for future work in this direction.

First investigations in the direction of biocompatibility were promising by proving that there are no residual endotoxin contaminations left from the bacterial production strain. Furthermore, no activation of blood platelets upon incubation with the crystalline adsorbent could be detected (Fig. S15 and S16, ESI†). Importantly, more in-depth investigations to prove complete hemocompatibility need to be performed for future application of this new material class.

In conclusion, we demonstrated the synthesis of macroscopic materials based on the bottom-up assembly of protein cages for blood purification applications. The resulting material shows stability and adsorption of three PBUTs. Furthermore, it was demonstrated that through the introduction of anchor sites, up to 96 water-insoluble aliphatic and phenylic molecules were incorporated inside the cavity of the ferritin protein cage. No decrease in biocompatibility could be found after these modifications. An increase in adsorption capacity due to the chemical modifications is observable. However, exclusively hydrophobic ligands are probably not optimal, since



- 10 F. C. Barreto, *et al.*, *Clin. J. Am. Soc. Nephrol.*, 2009, **4**, 1551–1558.
- 11 R. Vanholder, *et al.*, *Kidney Int.*, 2003, **63**, 1934–1943.
- 12 J. Jansen, J. Jankowski, P. R. Gajjala, J. F. M. Wetzels and R. Masereeuw, *Clin. Sci.*, 2017, **131**, 1631–1647.
- 13 T. L. Sirich, *et al.*, *Kidney Int.*, 2017, **91**, 1186–1192.
- 14 M. Madero, *et al.*, *Clin. J. Am. Soc. Nephrol.*, 2019, **14**, 394–402.
- 15 S. Yamamoto, *et al.*, *Sci. Rep.*, 2015, **5**, 14381.
- 16 C. Cosola, *et al.*, *Toxins*, 2021, **13**, 334.
- 17 V. Saar-Kovrov, W. Zidek, S. Orth-Alampour, D. Fliser, V. Jankowski, E. A. L. Biessen and J. Jankowski, *J. Intern. Med.*, 2021, **290**, 499–526.
- 18 M. Sternkopf, *et al.*, *Toxins*, 2019, **11**, 389.
- 19 D. Bergé-Lefranc, C. Vagner, R. Calaf, H. Pizzala, R. Denoyel, P. Brunet, H. Ghobarkar and O. Schäf, *Microporous Mesoporous Mater.*, 2012, **153**, 288–293.
- 20 V. Wernert, O. Schäf, H. Ghobarkar and R. Denoyel, *Microporous Mesoporous Mater.*, 2005, **83**, 101–113.
- 21 D. Pavlenko, D. Giasafaki, G. Charalambopoulou, E. van Geffen, K. G. F. Gerritsen, T. Steriotis and D. Stamatialis, *Sci. Rep.*, 2017, **7**, 14914.
- 22 S. Kato, K. I. Otake, H. Chen, I. Akpinar, C. T. Buru, T. Islamoglu, R. Q. Snurr and O. K. Farha, *J. Am. Chem. Soc.*, 2019, **141**, 2568–2576.
- 23 S. R. Sandeman, *et al.*, *Biomed. Mater.*, 2017, **12**, 035001.
- 24 P. D. Hempstead, S. J. Yewdall, A. R. Fernie, D. M. Lawson, P. J. Artymiuk, D. W. Rice, G. C. Ford and P. M. Harris, *J. Mol. Biol.*, 1997, **268**, 424–448.
- 25 K. Han, Y. Na, L. Zhang and F. A. Tezcan, *J. Am. Chem. Soc.*, 2022, **144**, 10139–10144.
- 26 B. S. Heater, Z. Yang, M. M. Lee and M. K. Chan, *J. Am. Chem. Soc.*, 2020, **142**, 9879–9883.
- 27 B. Maity, S. Abe and T. Ueno, *Nat. Commun.*, 2017, **8**, 14820.
- 28 A. Shaukat, E. Anaya-Plaza, N. K. Beyeh and M. A. Kostianinen, *Chem. – Eur. J.*, 2022, **28**, e202104341.
- 29 M. Künzle, T. Eckert and T. Beck, *J. Am. Chem. Soc.*, 2016, **138**, 12731–12734.
- 30 T. Tosha, H. L. Ng, O. Bhattasali, T. Alber and E. C. Theil, *J. Am. Chem. Soc.*, 2010, **132**, 14562–14569.
- 31 M. Lach, C. Strelow, A. Meyer, A. Mews and T. Beck, *ACS Appl. Mater. Interfaces*, 2022, **14**, 10656–10668.
- 32 J. Jankowski, *et al.*, *J. Clin. Invest.*, 2003, **112**, 256–264.
- 33 M. Hida, Y. Aiba, S. Sawamura, N. Suzuki, T. Satoh and Y. Koga, *Nephron*, 1996, **74**, 349–355.
- 34 L. Lu and J. T. W. Yeow, *Mater. Des.*, 2017, **120**, 328–335.
- 35 D. Pavlenko, D. Giasafaki, G. Charalambopoulou, E. van Geffen, K. G. F. Gerritsen, T. Steriotis and D. Stamatialis, *Sci. Rep.*, 2017, **7**, 14914.

